Recent Progress in Mössbauer Studies of Iron-Based Spinel Oxide Nanoparticles

Jana K. Vejpravova

1 Introduction

Mössbauer spectroscopy (MS) is the γ-ray recoilless-free nuclear resonance spectroscopy named after Rudolph Mössbauer who received the Nobel Prize for Physics in 1961 for this discovery [1]. This method serves as a powerful tool for investigation of the oxidation state, local crystallographic environment and orientation of the magnetic moments in the absorbing sample through the interactions of the absorbing nuclei with its surrounding, called the hyperfine interactions [2]. The MS experiment has two options by means of a radioactive source: conventional radioactive isotope, which will be discussed further in detail, and synchrotron radiation [3, 4]. The energy-domain MS illuminates the nuclear hyperfine structure directly from the

Preface
When being asked to contribute to this book, my idea was to discuss the peculiarities in understanding magnetic behaviour of nanoscale oxide magnets, in particular the relevance of the classical and quantum pictures featuring their magnetic properties. However, in November 2018, my great friend and colleague Daniel Nižňanský passed away. He attracted me to the fascinating field of nanomagnetism, and in particular, he always contributed significantly with his enormous expertize in synthesis and Mössbauer spectroscopy of fine particles of magnetic oxides. In memory of his great contribution to the magnetic nanoparticle research, I will provide current state of the art in this field from the perspective of applying Mössbauer spectroscopy techniques to magnetic spinel oxide nanoparticles. At this point, I would like to express my great thanks to my outstanding students and colleagues: Barbara Pacáková, Simona Kubíčková and Alice Mantlíková who did an excellent job and substantial advancement of the field during their doctoral studies. Finally, my great thanks belong to Puerto Morales, Alejandro Gomez Roca, Gorka Salas, Carla Cannas, Marco Sana, Valentina Mameli, Dominika Zakutna and Anton Repko for unforgettable collaboration and precious inputs on various aspects related to magnetic nanoparticles.

J. K. Vejpravova (✉)
Department of Condensed Matter Physics, Charles University, Prague, Czech Republic
e-mail: jana@mag.mff.cuni.cz

A. G. Roca et al. (eds.), *Surfaces and Interfaces of Metal Oxide Thin Films, Multilayers, Nanoparticles and Nano-composites*,
https://doi.org/10.1007/978-3-030-74073-3_1

absorption/emission positions of the resonance line, while the time-domain MS reflects the hyperfine structure due to the coherent process of nuclear resonant forward scattering. The time-domain MS, also called the spectrum of quantum beats of nuclear forward scattering, is typically carried using synchrotron radiation. In 1986, Gerdau et al. introduced the nuclear resonant spectroscopy in the time domain [5], and since then, this experimental technique has been intensively developed [5, 6]. Because synchrotron radiation has the advantages of excellent collimation, high brilliance, pulsed structure and close-to-ideal polarization, the experiments can be carried in both the energy and the time domain [3, 5, 7–10]. A unique study of Ni nanoparticles using the time-domain MS may serve as an interesting example [11].

However, the conventional energy-domain MS is a very well-established tool in the magnetic NP research, and from last two decades of twentieth century, there have been many substantial contributions, e.g. [12–17].

This chapter aims to present a recent progress in the field within last ~ 10 years on a friendly level. In particular, the important results on spinel ferrite NPs with a complex internal structure, including core–shell NPs, are highlighted. After a brief introduction, an up-to-date insight into the core–shell phenomenon of fine magnetic NPs is given, followed by an overview of the MS of magnetic NPs. The multifaceted term—a "core–shell" NP—is discussed from the perspective of chemical composition, and structural and spin order, which can be addressed by the MS very efficiently. The uniqueness of the MS is also placed in context of other methods used for investigation of magnetic NPs. The next section summarizes a collection of recent works carried out on "magnetic", "structural" and "chemical" core–shell NPs. The importance of a collective response in NP ensembles and its impact on the MS will be also briefly addressed. Finally, future prospects and possible innovative applications of spinel oxide NPs are outlined.

2 Magnetic Nanoparticles—The Core–Shell Phenomenon

It is a well-known fact that magnetic domains are created in crystals with ferromagnetic or ferrimagnetic ordering in order to decrease the magnetostatic energy that is associated with the dipolar fields. The creation of the domains depends on the competition between the reduction of the magnetostatic energy and the energy required to form the domain walls separating the adjacent domains. The size of the domain wall is a balance between the exchange energy that tries to unwind the domain wall and the magnetocrystalline anisotropy with the opposite effect.

In magnetic NPs (literally speaking in close to spherical nanocrystals with a mean diameter below ~ 100 nm), the typical dimensions are comparable with the thickness of the domain wall, and thus below a critical diameter, d_{crit}, the NP becomes a single domain. The critical diameter was proposed by Ch. Kittel [18, 19] in the form:

$$d_{crit} = \frac{9\sqrt{A_{ex}K_u}}{\mu_0 M_S^{\,2}} \tag{1}$$

where M_s is the saturation magnetization, A_{ex} and K_u are the exchange and uniaxial anisotropy constants, respectively. It is clear that the d_{crit} is material specific and ranges from few tens of nm in magnetic oxides to almost micrometre in hard rare earth-based magnets.

In magnetic NPs reaching the single-domain limit, magnetic properties are represented by a classical magnetic moment in the order of ~ 10^3–10^5 Bohr magnetons. Consequently, paramagnetic-like behaviour can be observed even below the T_c of the bulk material. The phenomenon is known as superparamagnetism (SPM) [20], while the magnetization reversal in the low temperature limit (in the so-called blocked state) has been introduced by Stoner and Wohlfarth [21]. Nevertheless, the macrospin approach neglects possible spin structure inside the NP. Decreasing the NP size, the numbers of atoms located at the surface (surface atoms) increases with respect to the all atoms, and at some defined size, surface atoms dominate the volume atoms. The atoms at the surface exhibit lower coordination number due to breaking of lattice symmetry at the surface proximity. Moreover, the exchange bonds are broken resulting in the spin disorder and frustration having consequences such as lowering of the saturation magnetization and/or lack of saturation in the high magnetic field [22, 23].

Already in 60-ties of the last century, the lower saturation magnetization of the NPs was identified, and several works tried to explain this feature considering the presence of a nonmagnetic layer (also termed magnetically "dead layer") [12] or presence of hydrogen in the lattice. In 1971, J. M. D. Coey [22, 23] suggested that the noncollinearity of the spins in NPs is responsible for the lower saturation magnetization and proposed the famous "core–shell" model of the NP.

In this case, the terms "core" and "shell" are related to a different spin arrangement in a model NP particle, which consists of a core with the bulk-like magnetic structure and a shell, where the spins are canted at random angles to the surface, giving rise to the so-called spin canting angle (please see Fig. 1, panel (a)). The spin canting angle depends on the number of the magnetic nearest neighbours connecting with the reduced symmetry and dangling bonds. This theoretical model was supported by the experimental evidence of the persistence of the 2nd and 5th absorption line in In-Field Mössbauer Spectroscopy (IFMS) pointing to the noncollinearity of some spins with the applied magnetic field. However, the same time he also pointed out that the possibility of some canting of the ions in the interior cannot be excluded.

In 1976, Morrish et al [24] tried to verify the Coey's model by inspection of a circular maghemite NPs with ^{57}Fe-enriched surface; however, the proof of enriching only the surface had not been given. Furthermore, it has to be noted that the enriching (thus further chemical treatment) usually induces additional disorder in the surface layer. They observed the broadening of the lines and the difference of the peak position of the 1st/6th line and 2nd/5th line, attributed to the lower effective field

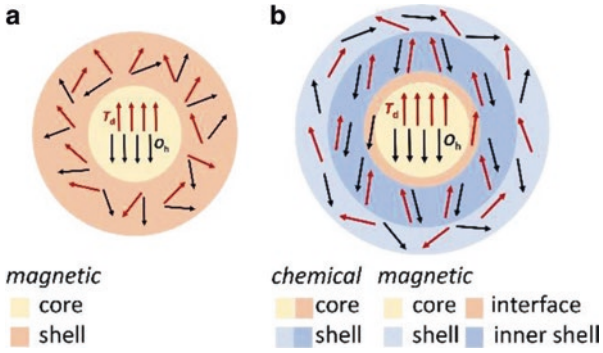

Fig. 1 Scheme of a core–shell model as suggested by Coey and termed "magnetic" in this chapter, adopted to a spinel ferrite NP (**a**) and a possible complex spin structure of a "chemical" core–shell NP of a spinel ferrite (**b**). Please note the interface between the inner and outer spinel phases. Illustration of a crystallographic (dis)order is omitted for clarity in both panels

that they connected with the surface spins. Up to date, there have been several studies with rather contrary results. Some studies suggested increase of the spin canting angle with decreasing particle size [17, 24]. Moreover, the same studies also investigated the influence of interparticle interactions (through the dilution of the samples in a polymer matrix) with no significant effect on the spin canting angle.

On the other hand, there are several works showing that the relative crystallinity of the NP is more important [24–27]. For example, Morrish et al [24] compared the maghemite NPs with different particle size and relative crystallinity—the well-crystalline 7 nm NPs and 95 nm NPs with high degree of disorder (the crystalline part had a mean diameter ~ 30 nm). Their results suggested that the NP internal structure is important and must be considered in any analysis of the surface spin canting as they observed quite a small difference in the spin canting angle in the two samples. Morales et al [25] studied 100 nm maghemite NPs with different vacancy ordering and found out that the spin canting angle varied with the vacancy ordering, suggesting the spin canting is a volume effect. So far, the volume or surface nature of the spin canting has been still debated.

There has been also several theoretical studies trying to solve the presence of the surface effects [13, 28, 29]. For instance, Pankhurst et al [29] proposed that the complete spin alignment cannot be achieved in the iron(III) oxide NPs due to the large magnetic anisotropy constant. After few years, this theoretical suggestion was questioned by Hendriksen et al in 1994 [13] who measured the IFMS of frozen ferrofluids. The study revealed that the spin canting angle is independent of the initial orientation of the magnetic moments in the NPs with respect to the external field; thus, the origin of the spin canting cannot be explained by enhanced magnetic anisotropy.

In past decade, the role of structure and morphology of NPs became a strong argument in explaining the complexity of spin arrangement in the magnetic NPs. It has been reported that the magnetic properties of NPs mostly result from their

internal structure [14, 27, 30, 31], particle size distribution [32, 33] and/or interparticle interactions [15, 34].

Yet, correlation of the magnetic properties with the crystal structure or particle size is not as straightforward as it is generally believed. First, it is usually claimed that very small NPs exhibit high ratio of the surface to volume spins that lowers the resulting saturation magnetization, M_s [22, 23, 26]. However, several studies have shown smaller M_s for large NPs [35, 36]. Furthermore, it is a common practice to evaluate magnetic properties of NPs upon their size, which is a vague term when taking into account the fact that every experimental method such as X-ray Diffraction (XRD), Transmission Electron Microscopy (TEM) or magnetization measurements provides a "size" with a different physical meaning. For instance, the TEM determines only a specific projection of the physical size of a NP, d_{TEM}, without any deeper insight into its relative crystallinity. Thus, correlations of the d_{TEM} with the magnetic response of NPs is highly misleading, but it has been widely performed [35, 37].

Without doubts, the internal structural and spin arrangement play important role and their proper investigation is a crucial point in correlation of structural and magnetic parameters of the NPs with their magnetic properties related to their performance in applications.

With increasing availability of the advanced instrumental techniques and advancements in the data processing and analysis, the current trend is to drain maximum information from a specific technique taking into account its operation range by means of dimension and time (or frequency) as it is summarized in Fig. 2.

A great benefit of the MS is its elemental selectivity and a very local character of probing the sample. Nevertheless, when studying very small objects such as NPs, one has to consider that all sample parameters with a given distribution will introduce complexity to the resulting spectra. Vice versa, a complicated character of the sample can be tracked with the help of MS via the complex information encoded in the MS.

MS also has a very sharp location on the energy (frequency). Therefore, it is often impossible to use it as a single probe to structure of magnetism of the material. Besides the less common techniques operating on the same scale, such as nuclear magnetic resonance NMR [36] and neutron diffraction [38], the widely used methods for investigation of magnetic NPs are: transmission electron microscopy (TEM) including high-resolution TEM (HRTEM) and electron energy loss spectroscopy (EELS), X-ray diffraction (XRD), dynamic light scattering (DLS) and various magnetometries among which the volume methods (vibrating sample magnetometry—VSM, superconducting quantum interference device—SQUID) prevail. Some groups successfully applied X-ray Photoemission Spectroscopy (XAS) and Extended Absorption Fine Structure (EXAFS) to get more insight into the local coordination environment of the cations in the spinel lattice [39]. In addition, advanced studies based on small-angle X-ray and neutron scattering and X-ray Magnetic Circular Dichroism (XMCD) have been performed [40–44]. Magnetic microscopies and other microscale methods such as magnetic force microscopy (MFM) and micro-Hall or micro-SQUID magnetometries are rarely applied as they

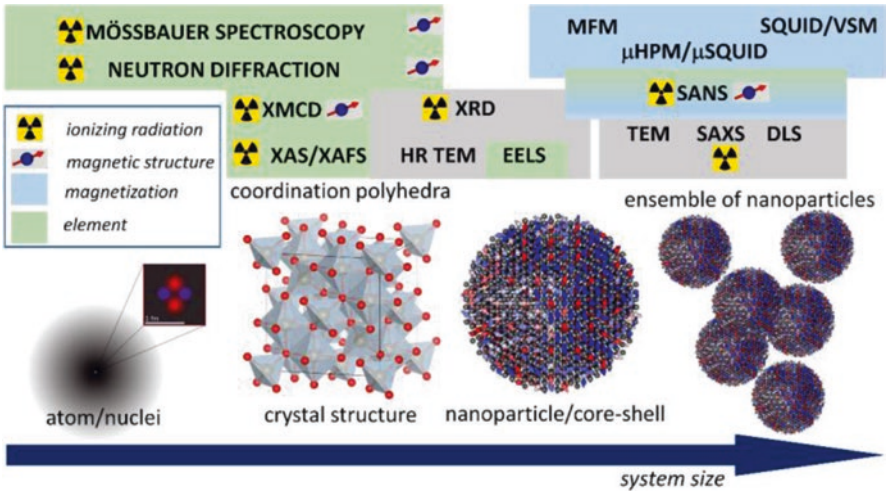

Fig. 2 Tentative diagram of the most common experimental methods used for investigation of magnetic nanoparticles in comparison to their typical operation range (given by the system size ranging from a single atom over a coordination polyhedron, unit cell, nanoparticle and ensemble of nanoparticles). The green blocks correspond to the methods, which are capable of elemental (chemical) selectivity, while the blue blocks mark the magnetometry-related methods, which enable detection of a certain sum of elementary magnetic moments. The grey blocks contain techniques with no specific elemental and magnetic selectivity; please note that for the spinel ferrites the Z values are very similar; thus, the electron density driven contrast is very low. Methods requiring ionizing radiation are marked with the "radiation" symbol. Methods which enable to resolve magnetic structure either on the level of a magnetic unit cell or on the level of a single particle are labelled by a "spin" symbol

require positioning of the NPs on a flat surface or a microprobe, respectively, and a signal from a single NP can be recorded [45, 46]. However, the techniques have very limited usage for understanding the complex structural and spin architectures within a single magnetic NP.

At this point, one has to revisit the meaning of the core–shell term. In the original concept by Coey, the core–shell is related to a different spin structure of the two parts of a single NP. In last few years, the so-called bimagnetic core–shell spinel oxide NPs have been explored intensively, namely due to their great performance in magnetic fluid hyperthermia [47]. In such NPs, one has to keep in mind that are in principle three different possibilities of understanding the core–shell phenomenon. First, the chemical composition varies across the NP volume; the core is composed of a different spinel ferrite than the shell, and a kind of "chemical core–shell" structure can be introduced. The bimagnetic core–shell NPs are typically prepared by a seed-mediated growth, which means that the second spinel ferrite phase (shell) is grown on a different spinel ferrite NP (core). However, the core has already a certain amount of structural disorder at the surface [30]. Consequently, a kind of internal interface within a single NP is formed and another structurally disordered layer forms in the proximity of the NP surface. Consequently, quite complex "structural

core–shell" arrangement can be observed. Keeping in mind the already complex "structural core–shell" situation, the final arrangement of magnetic moments in a "magnetic core–shell" perspective may become very complex due to the structural disorder at the inner interface and at the outer shell (please see the Fig. 1, panel (b)). Coming back to the common characterization techniques, the information they provide is usually related to one of the possible core–shell concepts. In this context, the MS (except photoelectron spectroscopies, which have limited usage due to very low penetration depth) is the only one providing information about the Fe valence. Moreover, a great challenge nowadays is to understand the MS experiments on the bimagnetic core–shell NPs to give more insight into all types of core–shell arrangement. In this vein, advanced MS studies profiting from temperature- and magnetic field-dependent experiments are needed. The most important aspects will be summarized in the next section.

3 MS of Magnetic NPs—Fundamentals

The small NPs exhibit relaxation time in order of 10^{-9} s that is close to the time window of the MS (10^{-8} s). It allows us to study the relaxation of the NPs by means of MS. Furthermore, the big advantage of the MS is that it is not restricted to the well-crystalline samples, and thus, all kinds of spinel ferrite NPs can be investigated using MS. An overview of the essential information embedded in the parameters of the spectra (position, intensity and profile) is given in Fig. 3, panel (a).

Below the blocking temperature T_B, NPs are in blocked state, thus the relaxation across the energy barrier is negligible, and the magnetically split spectra (evolved in sextet) are observed in the MS spectra. However, the macrospin fluctuates around the direction of the magnetization easy axis resulting in the so-called collective magnetic excitations that reduces the value of B_{hf} to resulting B_{obs} according to the equation:

$$B_{\mathrm{obs}} = B_0\left(1 - \frac{k_B T}{2K_{\mathrm{eff}}V}\right), \tag{2}$$

where B_0 is the B_{hf} without the effect of the collective magnetic excitations. The maximum reduction is found to be around 5—15%; the higher reduction leads to collapse of the magnetically split spectra to a broad singlet or doublet [48]. The temperature dependence of the B_{hf} in the blocked state is usually used for the determination of the K_{eff} of the NPs [2, 48, 49].

With increasing temperature, the thermal fluctuations dominate, leading to the collapse of the magnetically split spectra. The T_B determined from the MS is defined as the temperature at which half of the spectra area is magnetically split (sextet) and half of the spectra is in a doublet and/or singlet form.

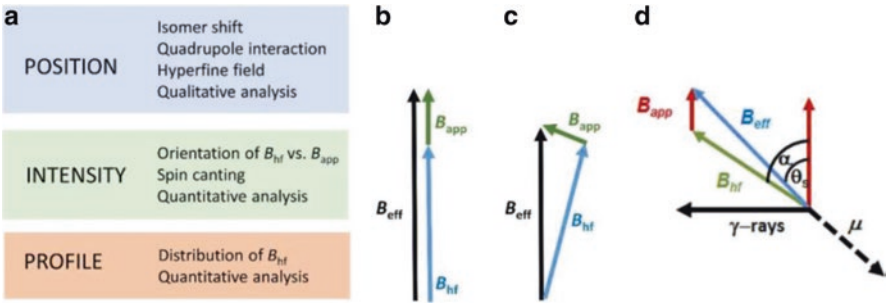

Fig. 3 Scheme of the parameters that can be derived from the refinement of MS (**a**). The simple sketch of behaviour of the B_{hf} in B_{app}: the parallel orientation of the B_{hf} with respect to B_{app} (**b**); the nonparallel direction of the B_{hf} with B_{app} that results in the smaller B_{eff} is depicted on the panel (**c**). The scheme of the spin canting angles derived from the perpendicular set-up of the IFMS (**d**). The θ_s is the angle between the B_{eff} and B_{app}; the α is the angle between the B_{hf} and the B_{eff}. The magnetic moment, μ, points antiparallel with the respect to the B_{hf} in the ferrite oxides

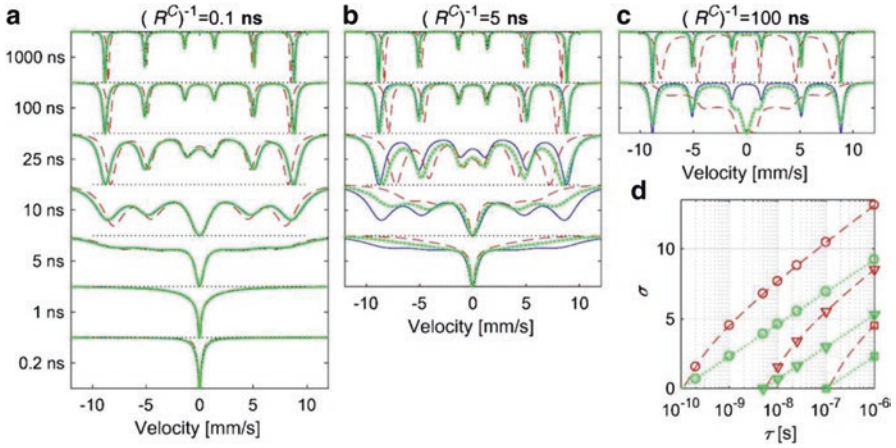

Fig. 4 Theoretical Mössbauer relaxation spectra for a hyperfine field switching between ±55 T and zero quadrupole interaction at SPM relaxation time calculated using the Blume–Tjon model [53] (blue, full lines), the three-level (S = 1) model (green, dotted lines) and the multilevel (S = 60) model (red, dashed lines). For the multilevel model, the relaxation time, τ, was calculated using the Brown model with the indicated values of R^{-1} ($\tau = R^{-1}f(\sigma)$;$\sigma = KV/k_BT$, where K is the anisotropy constant, V is the NP volume), and for the three-level model, it was calculated using the simplified Néel model. Panel (d) shows the results for the three-level model (green) and the multilevel model (red) for R^{-1} = 0.1 ns (circles), 5 ns (triangles) and 100 ns (squares). (Adopted from ref. [50])

A recent work by Fock et al [50] treated the problem of MS from the viewpoint of fluctuations of the direction of the magnetic hyperfine field by theoretical means. For noninteracting particles, the SPM relaxation results in the spectra consisting of a sum of a sextet and a doublet with a temperature-dependent area ratio. This is in accordance with the exponential dependence of the SPM relaxation time on the

particle size and temperature. An alternative interpretation of these features given by some authors is a first-order magnetic transition from a magnetically ordered state to a paramagnetic state [51]. However, the mistaken base of this interpretation is even corroborated by the fact that the doublet component has been found to transform to a magnetically split component when relatively small fields are applied, which excludes the formation of a paramagnetic state. In other cases, the spectra of magnetic NPs consist of sextets with asymmetrically broadened lines without the presence of doublets. It has been suggested that such spectra can be explained by a multilevel model [52], according to which the relaxation takes place between a large number of states. The authors suggested that the spectra with asymmetrically broadened lines (at least in some cases) should be better explained by the influence of magnetic interparticle interactions on the magnetic fluctuations, which brings the importance of the so-called real effects (size distribution, interparticle interactions) into play again.

Figure 4 gives an overview of calculated spectra using Blume–Tjon [53] and Jones–Srivastava model [52] in the three-level (S = 1) and multilevel (S = 60) conditions. While the character of the spectra is somewhat comparable, the increasing S (number of levels) in the multilevel model leads to decrease of the B_{hf}.

In the real systems, the particle size distribution generally results in the distribution of the relaxation time. Due to the exponential dependence of the relaxation time, the broad distribution of the B_{hf} is observed in these systems [49, 50].

In order to obtain some information about the possible core–shell spin structure, represented often by the so-called spin canting angle (angle between the B_{app} and B_{hf}/B_{eff} of a NP) that is usually attributed to the presence of the surface spins, the in-field MS (IFMS) is usually performed. However, the computation of the spin canting angle is not so obvious in spinel ferrite and bimagnetic spinel ferrite NPs, and the precise determination of its value is in most cases impossible.

Generally, there are two approaches, how the spin canting angle can be determined. First, the spin canting angle can be derived from the relative areas of the 2nd and 3rd absorption lines. For an arbitrary angle between the γ-rays and magnetic field, the resulted equation is:

$$3 : \frac{4\sin^2\theta_S}{1+\cos^2\theta_S} : 1, \tag{3}$$

where θ_s is the angle between the B_{hf} and the direction of γ- rays. This formula is only valid for the transitions from I = 3/2 to I = ½ levels, that is the case of the nucleus of ^{57}Fe. In the case of powder samples, the probability (thus the relative intensities) is proportional only to the square of the Clebsch–Gordan coefficients resulting in the 3:2:1:1:2:3 ratio [2].

It has to be noted that this approach can be inaccurate due to several reasons. First, the area of the absorption lines is affected by relative thickness of the sample, and the thick sample results in the saturation of the lines, thus affecting ratio of the line areas [54]. Second, the θ_s is the angle between the B_{eff} and B_{app} that does not

coincide with the orientation of the magnetic moment, μ, as is displayed in Fig. 3, panel (d).

In ferrite oxides, the μ of the nucleus is oriented antiparallel to the B_{hf} due to the negative Fermi contact term, others contributions can be neglected, and therefore, the size should be proportional to the value of the B_{hf}. If the external field is applied, the magnetic moment tends to align in parallel direction with the B_{app}. The B_{hf} will rotate as to be antiparallel with the μ. Therefore, even in B_{app}, the μ is antiparallel with the B_{hf}, not the B_{eff}. Determination of the angle from the area of the lines is related to the angle between the quantization axis and the direction of the γ-rays that is usually parallel with the B_{app}, as it is in spinel ferrites.

There are two possible experimental set-ups used for the IFMS. First, the B_{app} is applied parallel with the direction of the γ-rays (Fig. 3, panel (b)); the resulting equation is similar to the (2). Second, the B_{app} is applied perpendicularly to the direction of the γ-rays (Fig. 3, panel(c)), and the Eq. (2) converts to the:

$$4\left(\frac{2}{\sqrt{1+\sin^2\theta_S}}-1\right):1. \tag{4}$$

The second approach accounting for the nonzero angle between the B_{hf} and B_{app} that is physically relevant requires the measurements of both the zero-field spectrum together with the in-field spectrum, yielding the B_{hf} and B_{eff}, respectively. The spin canting angle is then given by the following expression:

$$\cos\alpha = \frac{B_{\mathrm{eff}}{}^2 - B_{\mathrm{app}}{}^2 - B_{hf}{}^2}{2B_{\mathrm{app}}B_{hf}}. \tag{5}$$

When studying spinel oxide NPs, one usually treats a whole ensemble of NPs. It has been demonstrated many times that especially the dense ensembles of magnetic NPs experience strong dipolar fields and the magnetization reversal in such systems is determined by the strength of the mutual interparticle interaction [32, 34, 55].

Based on the stochastic approaches, a simplified three-level stochastic model taking into account the magnetic anisotropy, precession and diffusion of uniform magnetization of single-domain particles was proposed by Chuev [56] in order to describe the MS of magnetic NPs in a weak magnetic field; results of his calculations are shown in Fig. 5. The MS obtained for the different geometries show clear differences, which are originated by the magnetic anisotropy, precession and diffusion of uniform magnetization of the NPs. The obvious polarization effects present in the theoretical spectra point to the fact that a relevant description of the experimental data containing randomly or partly oriented NPs (by means of their easy axis to the applied magnetic field) requires description based on the spectral parameter distributions.

Another example can be found in the recent work of Majetich et al. [57]. They have shown that multiparticle correlations, both parallel and perpendicular to the applied field, exist in ordered assemblies of NPs. By atomistic simulation, they have

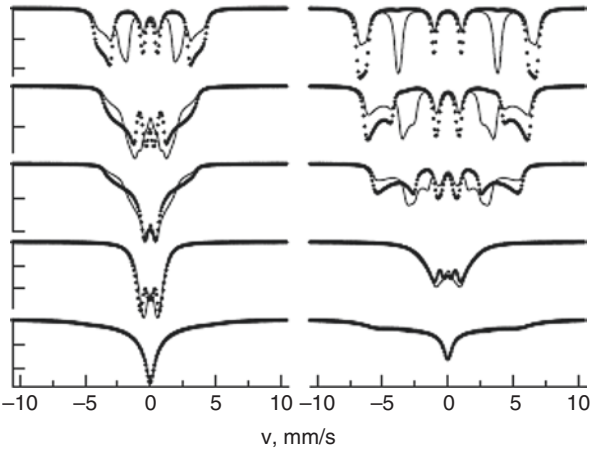

Fig. 5 IFMS of an ensemble of NPs for a transverse and longitudinal magnetic field geometry calculated using three-level relaxation model. The normalized field strength h = 0.01, 0.1, 0.5, 1 and 2 (from bottom to top). (Adopted from ref. [56])

revealed that the magnetic frustration in the shell, which may originate from Dzyaloshinskii–Moriya interactions (DMI) of Mn B site ions, leads to a modest amount of surface canting, which can act as a source of anisotropy.

Strong exchange coupling between the core and shell causes the core spins to cant, as well. In dense assemblies, magnetostatic interactions among the particles favour canting of the particle moments in the same direction. This coherent canting results in a so-called canted superferromagnet or canted supermagnet that collectively shows canted ferromagnetic behaviour.

In summary, the MS in principle provides a lot of information about the spin orientation in spinel ferrite NPs, and it is capable of reflecting real effects such as particle size distribution, internal and surface spin canting, and interparticle interactions. However, a careful analysis and a critical interpretation of the results are needed to obtain a realistic picture. Examples of exploring the chemical, structural and magnetic core–shell spinel ferrite NPs by MS are given in the next section.

4 Selection of Recent Studies

In this section, a selection of interesting works published within last ~ 10 years and going beyond the state of the art described previously is presented. Let me stress out that one can easily find few hundreds of research papers published within the last 10 years, which report on the application of MS on spinel ferrite NPs. However, most of the studies use ambient MS or temperature-dependent MS, providing only room temperature and 4.2 K or 77 K spectra. Majority of the works do not go beyond the knowledge established by the Mørup, Fiorani or Tronc and their successors, which means that the complex nature of the spectra due to the chemical, structural and magnetic disorder as well as nontrivial distribution of hyperfine parameters is not considered. The IFMS studies are also quite rare. Literally speaking, the MS

is mostly used as a reliable tool for determination of the iron valence and a complementary technique of phase analysis, e.g. to the XRD. Therefore, the aim of this section is to highlight the works with substantial progress in applying the MS to the spinel ferrite NPs. First, the iron oxide NPs with a complex internal structure are discussed. Then, other spinel ferrite NPs including chemically doped systems are presented. Finally, several studies of nominally chemical core–shell spine ferrite NPs with a very complex scenario of spin order are included.

4.1 Structural and Magnetic Properties of Spinel Ferrite NPs

Iron Oxide NPs

The most studied spinel ferrite in the form of NPs is magnetite, and the MS is usually used to confirm the presence of Fe^{2+}. However, it has been demonstrated many times that the magnetite NPs undergo a continuous topotactic oxidation to maghemite, and consequently, the structural arrangement of a real NP gains complexity.

The groups of Vejpravova and Morales focused on the question of spin disorder and spin canting in a series of highly uniform iron oxide NPs [27, 30, 58].

Selected samples with different relative crystallinity were investigated, also by the IFMS with B_{app} increasing from 0 to 6 T with the step of 1 T. The evolution of hyperfine parameters was determined with emphasis on the calculation of the spin canting angle. Finally, the resulting parameters were correlated with internal structure of the NPs, which was probed by HR TEM and XRD, and corroborated by the magnetic measurements. It has been pointed out that the value of the spin canting angle is strongly dependent on the approach used and exact value of the spin canting angle is disputable. The value of θs determined from the area under a peak is strongly dependent on the refinement procedure used. The value of α is derived from the values of B_{hf}, B_{eff} and B_{app}, where the B_{hf} is determined with considerable experimental error due to the fully overlapped sextets; thus, the resulting α is only estimative.

The well-crystalline samples with different particle diameter served as great candidates to solely correlate the resulting spin canting angle with the increasing particle size. The effect of the spin disorder is expected to be negligible in these samples. On the other hand, imperfections in internal structure of the NPs with different origin were observed in the two samples with identical TEM size. One sample can be viewed as a magnetic core–shell NP (Coey-like), where the disordered spins are located at the surface. The other sample possesses stacking faults that split the highly crystalline NP into at least two crystalline domains; therefore, the disordered spins are located in the whole volume of the NP, namely at the internal interfaces. For the first time, IFMS study of these two samples allows to disentangle the origin of the possible spin canting, but only in context of other characterization techniques.

For example, the normalized IFMS at 6 T did not reveal any significant differences in the profile for both samples, the asymmetric broadening at the lower values of the B_{hf} is pronounced and comparable in both spectra, and the θs and α values are identical within the experimental error. It has been demonstrated that a realistic orientation of spins with respect to the B_{app} can be obtained by measuring the evolution of the values of B_{eff} with increasing B_{app} that gives the complex behaviour of the spins in individual sublattices [27, 58]. Please note that the quite popular refinement of the MS by the Coey-like core–shell model has to be performed carefully as the values of the B_{eff} for the disorder (shell) spins are dependent on the orientation of the spins of the individual sublattices with respect to the B_{app} [27].

Another complex study by means of magnetic, XRD and MS studies on uniform magnetite/maghemite core–shell NPs was reported by Iyengar et al [59]. A very interesting aspect of this work is the use of vibrational spectroscopies (Raman and Fourier Transform Infrared Spectroscopy, FTIR), which clearly confirmed presence of magnetite and maghemite phases with a distribution of coordination polyhedral deformation. The fit of the MS to a core–shell model (magnetite/maghemite) enabled determination of the shell thickness.

Multicore γ-Fe_2O_3 nanoparticles were studied by Kamali et al [31]. They focused on the formation of a core–shell structure, consisting of multiple maghemite NPs as the core and silica as the shell. Low-temperature MS reveals the presence of pure maghemite NPs with all vacancies at the B sites. Surprisingly, the multicore γ-Fe_2O_3 NPs show similar magnetic behaviour comparing to the isolated particles of the same size. However, this conclusion in fact illustrates the importance of taking into account interparticle interactions present in all NP samples studies as powders.

A very detailed MS study of core/shell Fe_3O_4/γ-Fe_2O_3 NPs has been published by Kamzin et al [60]. The phase composition, the structure of cores and shells, and the dependences of the shell thickness on the fabrication technique were determined for magnetite core with a fixed size (8 nm) and γ-Fe_2O_3 shells of a varying thickness (from one to five nm). It was found that the surface layer and the "bulk" of these shells had different magnetic structures. This difference was attributed either to the frustration of spin magnetic moments or to the formation of a canted spin structure in the surface layer. The intermediate layer between the core and the shell is likely to be in a spin-glass state. Both the Mössbauer spectra and the reconstructed B_{eff} distributions have characteristic features suggesting either a narrow size distribution of the studied NPs or the existence of relaxation processes in these NPs.

A work by Kalska-Szostko et al [55] pointed out to the importance of intra- and interparticle interactions as evidenced by a study carried out on ferrite magnetic NPs with core–shell structures obtained in two-step preparation process. The interesting aspect of this study is the comparison between two "inverse" core–shell structures: the magnetite shell on maghemite core and *vice versa*.

Beside the spinel iron oxide core–shell NPs, some studies report on structures composed of different iron oxides. In this case, the system is in principal homogeneous by means of elemental composition, but it can be viewed as a "structural" core–shell as the two iron oxide phases have a different lattice symmetry. Please note that the magnetite/maghemite core–shell NPs can be in principle viewed in the

same way; however, both phases form a spinel structure, in spite of a different occupation of the lattice sites.

An example of such a formally "structural" core–shell system has been studied by Kamzin et al [61]. FeO/Fe_3O_4 nanoparticles were synthesized by thermal decomposition method and the MS of the phase composition of the synthesized nanoparticles clearly revealed the simultaneous presence of three phases: magnetite Fe_3O_4, maghemite γ-Fe_2O_3 and wustite FeO. This work also confirmed a scenario proposed for "simple" iron oxide NPs [30] that the saturation magnetization is not the only factor governing the SAR, and the efficiency of heating of magnetic FeO/Fe_3O_4 nanoparticles may be increased by enhancing the effective anisotropy.

Another example is the work by Lak et al [62]. Size-dependent structural and magnetic properties of FeO–Fe_3O_4 NPs prepared *via* decomposition of iron oleate were investigated. The authors applied many different experimental techniques (HR TEM, XRD, MS and magnetization measurements) and received a complete picture of the internal structural and spin order. Based on that the authors provided a model describing the phase transformation from a pure Fe_3O_4 phase to a mixture of Fe_3O_4, FeO and interfacial FeO–Fe_3O_4 phases with increasing NP size. The reduced magnetic moment in FeO–Fe_3O_4 NPs was attributed to the presence of differently oriented Fe_3O_4 crystalline domains in the outer layers and paramagnetic FeO phase. Interestingly, the exchange bias energy was found to dominate in the magnetization reversal mechanism, and the SPM blocking temperature in FeO–Fe_3O_4 NPs depends strongly on the relative volume fractions of FeO and the interfacial phase. This work is another great example of a system with a very complex structural and magnetic core–shell structure, however, composed of two elements only.

Other Spinel Ferrite NPs

The situation becomes even more complex when the spinel structure contains another element; the most common are cobalt and manganese ferrites. Nevertheless, the first complex MS studies have been reported since 90-ties of the last century. The most discussed point is the degree of the spinel inversion, which was addressed by many groups in cobalt, zinc and copper ferrite NPs [38, 63–70]. A general problem (already discussed in Sect. 2) is how to rigorously disentangle the effect of degree of inversion and the spin canting phenomenon. Though, the information about the internal structure of the NPs obtained from the XRD or TEM enables one to interpret the character of the MS and IFMS under the realistic approximations, as shown, e.g., in [63] (please see Fig. 6).

Even more complex results have been reported for spinel ferrites upon doping [71–74]. Cu-doped cobalt ferrite was explored by Batoo et al [71]. MS at room temperature shows two ferrimagnetically relaxed Zeeman sextets. The dependence of MS parameters such as isomer shift, quadrupole splitting, line width and hyperfine magnetic field on Cu^{2+} ion concentration is in line with the continuously changing magnetic parameters, such as effective anisotropy constant.

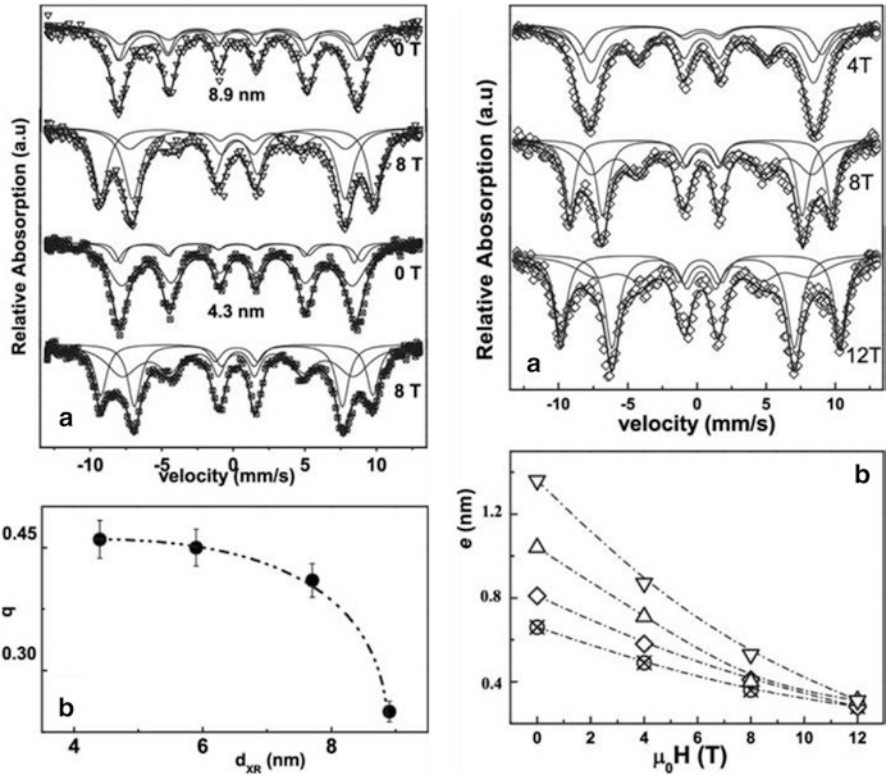

Fig. 6 (**a**) MS at 4.2 K of samples with a different particle diameter in zero and 8 T applied fields. All spectra are fitted with three magnetic sextets. (**b**) Mossbauer spectra at 4.2 K of the sample with diameter of 4.3 nm at the indicated fields. (**c**) Fraction of Fe ions belonging to the outer shell of canted spins as a function of the particle diameter. (**d**) Thickness of the disordered spins surface layer as a function of applied field for the samples with a different diameter. (Adopted from ref. [63])

Complex magnetic properties resulting from core–shell interactions in nanosized $Ni_{0.25}Co_{0.25}Zn_{0.5}Fe_2O_4$ synthesized by chemical coprecipitation method were treated by Lakshmi et al [72]. The authors observed exchange bias phenomenon, and they suggested that the effect is arising from the core–shell interaction. The observed variation in coercivity and exchange bias field suggested that only the core is affected by the cooling field. The authors used complementary IFMS regimes: zero-field-cooled and field-cooled and parallel and perpendicular orientation of the γ rays with respect to the B_{app}, respectively. Careful analysis of the spectra revealed that 70% of the spins are in the shell. The system can be modelled as an ordered core with conventional collinear arrangement of spins at the A and B sites and a canted, highly frustrated surface. The effects observed are comparable to those obtained in nanogranular systems comprising ferromagnetic particles embedded in an antiferromagnetic matrix. The large volume fraction of surface spins completely isolates

the cores so that the entire ensemble behaves as a system of nearly perfectly noninteracting particles. However, the NPs were prepared by coprecipitation, and consequently, they have significant size distribution and level of structural disorder therefore all absolute values should not be considered on a too quantitative basis. The spinel lattice can accommodate other elements, such as lanthanides. In the work by Burianova et al [73, 74], the authors prepared a series of cobalt ferrite NPs doped with lanthanum by microemulsion method. Detailed IFMS studies were performed to determine spin canting angles and cation distribution within the spinel network. Canting angles up to 40 degrees in the La-doped samples were observed. The presence of the spin surface effects was also supported by magnetic measurement as the magnetization did not saturate even in considerably high magnetic fields (7 T). The observed features originated from the surface spin disorder were explained in the simplified frame of the magnetic core–shell model; however, the importance of local strains and structural disorder due to the La doping is also proposed.

4.2 Chemical Core–Shell Spinel Ferrite Nanoparticles

It was demonstrated in the previous section that the core–shell phenomenon is a much intricate concept outreaching the common view of a NP composed of a core and a shell, each of a different material or with a different spin alignment. In a general context, one can distinguish between chemical, structural and magnetic core–shell structures. With increasing number of elements in the spinel oxide phases and artificially formed "chemical" core–shell NPs with multiple internal regions with a different composition and structural/spin order, rigorous understanding limits to "mission impossible". As already mentioned, the MS has quite limited information ability when used as a single probe of chemistry, structure and magnetism. Therefore, realistic approximations profiting from a robust methodological approach must be considered.

A showcase study of bimagnetic core–shell NPs composed of cobalt ferrite core and iron oxide or manganese ferrite shell was reported by the group of Cannas and co-workers [75]. They obtained a clear evidence of the chemical, structural and magnetic core–shell formation indirectly by comparing the MS of the core–shell samples and an *ad hoc* mechanical mixture and directly by mapping the NP's chemical composition by EELS. Chemical-sensitive electron tomography revealed detailed three-dimensional images of the NPs with a subnanometre spatial resolution.

Another great example featuring a maximum synergy of the experimental and theoretical methodologies has been recently released by the York group [57]. In my opinion, the work represents the benchmark by means of exactness for all future studies on spinel ferrite NPs.

The study focuses on intraparticle and interparticle effects in Fe_3O_4/Mn-ferrite core/shell structures [57]. The authors demonstrated that strong DMI can lead to magnetic frustration within the shell and cause canting of the net NP macrospin. The chemical composition and structural composition explored with the help of

MS, XAS and XMCD were used to determine the configuration on the Mn sites. In addition, polarized SANS experiments were performed and revealed parallel and perpendicular magnetic correlations, suggesting multiparticle coherent spin canting in an applied field. Atomistic simulations have revealed the underlying mechanism of the observed spin canting (for a graphical representation of the model, please see Fig. 7). The results show that strong DMI can lead to magnetic frustration within the shell and cause canting of the net particle moment. Nevertheless, strong exchange coupling between the core and shell also causes the core spins to cant. In ensembles of NPs, the magnetostatic interactions cause the NP magnetic moments to cant in the same direction giving rise to a superferromagnet or canted supermagnet state. These results have illuminated how core–shell NP systems can be engineered for spin canting across the whole volume of the particle, rather than solely at the surface. In context of practical applications, the local strains and DMI could affect the response of NP spins to the high-frequency magnetic field in the magnetic fluid hyperthermia, as suggested previously [30].

5 Conclusions and Future Prospects

Within the last decade, the research on spinel oxide NPs has been mostly motivated by fine tuning of the NPs for biomedical applications. It has been demonstrated that the MS is a great tool for addressing various aspects of spinel oxide NPs. Nevertheless, the power of MS is even multiplied when the results are put in context of other probes operating on different structural and magnetic scales and corroborated by theoretical calculations. In particular, the complex nature of the structural and magnetic ordering within a single NP as well as the mesoscopic effects (size distribution, interparticle interactions) can be revealed by the advanced experiments

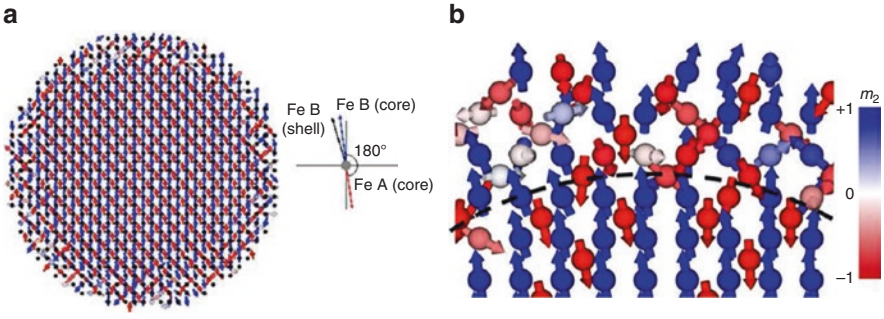

Fig. 7 (**a**) Visualization of the simulated spin configuration of a Fe_3O_4 core and $Mn(Fe_{1-x}Mn_x)_2O_4$ shell including DMI interactions on Mn B sites. The simulation temperature is set at 0 K in a 0.1 T externally applied field along the [001] crystal direction. (**b**) Enlargement of a region of panel (**a**), with dashed line to show the boundary between core and shell. Colour bar indicates direction of spin magnetization (blue, +1 or red, −1) on the spin sites. (Adopted from ref. [57])

and data analysis. Thanks to much deeper understanding of the complexity on the level of a single NP, some novel terms such as "intraparticle" interactions, "internal structure" and "nanointerface" have been introduced. In this chapter, the confusions in understanding the "core–shell" phenomenon were mitigated by definition of a chemical, structural and magnetic core–shell NPs, and the role of internal interfaces has been emphasized.

Certainly, the recent trends in understanding the fundamentals of NP magnetism include multifaceted experimental investigations in context of theoretical simulations capable of the complex system description. Such rigorous approach opens door to better understanding the mechanism underlying large variations in performance seen in magnetic NPs used for magnetic hyperthermia. For example, instead of tuning the common particle parameters (phase composition, size), the role of surface and internal spin frustration due to either DMI or local strains could affect the response of entire NP to alternating magnetic fields, which would impact the heat generation.

Being affected with the current situation of COVID-19 pandemic disease, the role of the tiny magnets in the detection and even therapeutic protocols should not be overlooked as they are widely present in numerous commercial kits for RNA and DNA separation. For example, a NP-based simple viral RNA detection for a RT-PCR molecule diagnosis has been reported very recently [76]. The development of high-impact methodologies based on the spinel oxide (ferrite) NPs can both speed up the detection procedures and make them very efficient by means of miniaturization. Therefore, the new wave of magnetic NP research may rise due to the great promises of their utilization in the revolutionary diagnostic technologies. Nevertheless, understanding the fundamentals of their magnetic performance is a must for a targeted development in this direction.

Acknowledgments This work was supported by the European Research Council (ERC-Stg-716265) and Ministry of Education, Youth and Sports of the Czech Republic under Operational Programme Research, Development and Education, project Carbon allotropes with rationalized nanointerfaces and nanolinks for environmental and biomedical applications (CARAT), number CZ.02.1.01/0.0/0.0/16_026/0008382.

References

1. R.L. Mössbauer, Kernresonanzfluoreszenz von Gammastrahlung in Ir191. Z. Phys. **151**, 124–143 (1958). https://doi.org/10.1007/BF01344210
2. T. Glaser, in *Mössbauer Spectroscopy and Transition Metal Chemistry. Fundamentals and Applications*, ed. by P. Gütlich, E. Bill, A. X. Trautwein, (Springer, Berlin, Heidelberg, 2011)
3. E. Gerdau, R. Rüffer, H. Winkler, et al., Nuclear Bragg diffraction of synchrotron radiation in yttrium iron garnet. Phys. Rev. Lett. **54**, 835–838 (1985). https://doi.org/10.1103/PhysRevLett.54.835
4. G.V. Smirnov, U. van Bürck, A.I. Chumakov, et al., Synchrotron Mössbauer source. Phys. Rev. B **55**, 5811–5815 (1997). https://doi.org/10.1103/PhysRevB.55.5811

5. M. Seto, R. Masuda, S. Higashitaniguchi, et al., Synchrotron-radiation-based Mössbauer spectroscopy. Phys. Rev. Lett. **102**, 217602 (2009). https://doi.org/10.1103/PhysRevLett.102.217602
6. T. Li, X. Zhang, The prime beat components extraction method for the time spectra analysis of nuclear resonant forward scattering. Materials, **12**(10), 1657 (2019). https://doi.org/10.3390/ma12101657
7. J.B. Hastings, D.P. Siddons, U. van Bürck, et al., Mössbauer spectroscopy using synchrotron radiation. Phys. Rev. Lett. **66**, 770–773 (1991). https://doi.org/10.1103/PhysRevLett.66.770
8. E. Gerdau, R. Rüffer, R. Hollatz, J.P. Hannon, Quantum beats from nuclei excited by synchrotron radiation. Phys. Rev. Lett. **57**, 1141–1144 (1986). https://doi.org/10.1103/PhysRevLett.57.1141
9. R. Masuda, K. Kusada, T. Yoshida, et al., Synchrotron-radiation-based Mössbauer absorption spectroscopy with high resonant energy nuclides. Hyperfine Interact. **240**, 1–6 (2019). https://doi.org/10.1007/s10751-019-1672-x
10. M. Seto, R. Masuda, S. Higashitaniguchi, et al., Mössbauer spectroscopy in the energy domain using synchrotron radiation. J. Phys. Conf. Ser. **217**, 012002 (2010). https://doi.org/10.1088/1742-6596/217/1/012002
11. R. Masuda, Y. Kobayashi, S. Kitao, et al., 61 Ni synchrotron radiation-based Mössbauer spectroscopy of nickel-based nanoparticles with hexagonal structure. Sci. Rep. **6**, 6–10 (2016). https://doi.org/10.1038/srep20861
12. E. Tronc, P. Prene, J.P. Jolivet, et al., Magnetic behaviour of γ-Fe2O3 nanoparticles by mössbauer spectroscopy and magnetic measurements. Hyperfine Interact. **95**, 129–148 (1995). https://doi.org/10.1007/BF02146310
13. P.V. Hendriksen, S. Linderoth, C.A. Oxborrow, S. Morup, Ultrafine maghemite particles. II. the spin-canting effect revisited. J. Phys. Condens. Matter **6**, 3091–3100 (1994). https://doi.org/10.1088/0953-8984/6/16/014
14. S. Mørup, E. Brok, C. Frandsen, Spin structures in magnetic nanoparticles. J. Nanomater. **2013** (2013). https://doi.org/10.1155/2013/720629
15. S. Mørup, M.F. Hansen, C. Frandsen, Magnetic interactions between nanoparticles. Beilstein J. Nanotechnol. **1**, 182–190 (2010). https://doi.org/10.3762/bjnano.1.22
16. E. Tronc, P. Prené, J.P. Jolivet, et al., Spin canting in γ-Fe2O3 nanoparticles. Hyperfine Interact. **112**, 97–100 (1998)
17. P. Prené, E. Tronc, J.P. Jolivet, et al., Mössbauer investigation of non-aggregated γ-Fe2O3 particles. Hyperfine Interact. **93**, 1409–1414 (1994). https://doi.org/10.1007/BF02072885
18. J. Stöhr, H.C. Siegmann, *From Fundamentals to Nanoscale Dynamics* (Springer-Verlag, Berlin, Heidelberg, 2006)
19. B.D. Cullity, C.D. Graham, *Introduction to Magnetic Materials* (Wiley, Hoboken, 2008)
20. W.F. Brown, Thermal fluctuations of a single-domain particle. Phys. Rev. **130**, 1677–1686 (1963). https://doi.org/10.1103/PhysRev.130.1677
21. E.C. Stoner, E.P. Wohlfarth, A mechanism of magnetic hysteresis in heterogeneous alloys. Philos. Trans. R. Soc. Lond. Ser. A Math. Phys. Sci. **240**, 599–642 (1948). https://doi.org/10.1098/rsta.1948.0007
22. J.M.D. Coey, Noncollinear spin arrangement in ultrafine ferrimagnetic crystallites. Phys. Rev. Lett. **27**, 1140–1142 (1971). https://doi.org/10.1103/PhysRevLett.27.1140
23. J.M.D. Coey, D. Khalafalla, Superparamagnetic γ-Fe2O3. Phys. Status Solidi **11**, 229–241 (1972). https://doi.org/10.1002/pssa.2210110125
24. A. Morrish, K. Haneda, P. Schurer, Surface magnetic structure of small γ-Fe2O3 particles. J. Phys. Colloques. **37**, C6-301–C6-305 (1976). https://doi.org/10.1051/jphyscol:1976663
25. M.P. Morales, S. Veintemillas-Verdaguer, M.I. Montero, et al., Surface and internal spin canting in γ-Fe2O3 nanoparticles. Chem. Mater. **11**, 3058–3064 (1999). https://doi.org/10.1021/cm991018f
26. A.G. Roca, D. Niznansky, J. Poltierova-Vejpravova, et al., Magnetite nanoparticles with no surface spin canting. J. Appl. Phys. **105**, 114309 (2009). https://doi.org/10.1063/1.3133228

27. S. Kubickova, D. Niznansky, M.P. Morales Herrero, et al., Structural disorder versus spin canting in monodisperse maghemite nanocrystals. Appl. Phys. Lett. **104**, 223105 (2014). https://doi.org/10.1063/1.4881331
28. H. Kachkachi, A. Ezzir, M. Noguès, E. Tronc, Surface effects in nanoparticles: application to maghemite -Fe O. Eur. Phys. J. B. **14**, 681–689 (2000). https://doi.org/10.1007/s100510051079
29. Q.A. Pankhurst, R.J. Pollard, Origin of the spin-canting anomaly in small ferrimagnetic particles. Phys. Rev. Lett. **67**, 248–250 (1991). https://doi.org/10.1103/PhysRevLett.67.248
30. B. Pacakova, S. Kubickova, G. Salas, et al., The internal structure of magnetic nanoparticles determines the magnetic response. Nanoscale **9**, 5129 (2017). https://doi.org/10.1039/c6nr07262c
31. S. Kamali, E. Bringas, H.-Y. Hah, et al., Magnetism and Mossbauer study of formation of multi-core gamma-Fe2O3 nanoparticles. J. Magn. Magn. Mater. **451**, 131–136 (2018). https://doi.org/10.1016/j.jmmm.2017.10.102
32. B. Pacakova, A. Mantlikova, D. Niznansky, et al., Understanding particle size and distance driven competition of interparticle interactions and effective single-particle anisotropy. J. Phys. Condens. Matter **28**, 206004 (2016). https://doi.org/10.1088/0953-8984/28/20/206004
33. H.S. Dehsari, V. Ksenofontov, A. Moeller, et al., Determining magnetite/maghemite composition and core-shell nanostructure from magnetization curve for iron oxide nanoparticles. J. Phys. Chem. C **122**, 28292–28301 (2018). https://doi.org/10.1021/acs.jpcc.8b06927
34. D. Fiorani, D. Peddis, Understanding dynamics of interacting magnetic nanoparticles: From the weak interaction regime to the collective superspin glass state. J. Phys. Conf. Ser. **521**, 012006 (2014). https://doi.org/10.1088/1742-6596/521/1/012006
35. G. Salas, C. Casado, F.J. Teran, et al., Controlled synthesis of uniform magnetite nanocrystals with high-quality properties for biomedical applications. J. Mater. Chem. **22**, 21065–21075 (2012). https://doi.org/10.1039/c2jm34402e
36. S. Belaïd, S. Laurent, M. Vermeech, et al., A new approach to follow the formation of iron oxide nanoparticles synthesized by thermal decomposition. Nanotechnology **24**, 055705 (2013). https://doi.org/10.1088/0957-4484/24/5/055705
37. M. Estrader, A. Lopez-Ortega, I.V. Golosovsky, et al., Origin of the large dispersion of magnetic properties in nanostructured oxides: FexO/Fe3O4 nanoparticles as a case study. Nanoscale **7**, 3002–3015 (2015). https://doi.org/10.1039/c4nr06351a
38. V. Blanco-Gutierrez, E. Climent-Pascual, M.J. Torralvo-Fernandez, et al., Neutron diffraction study and superparamagnetic behavior of ZnFe2O4 nanoparticles obtained with different conditions. J. Solid State Chem. **184**, 1608–1613 (2011). https://doi.org/10.1016/j.jssc.2011.04.034
39. A. Kuzmin, J. Chaboy, EXAFS and XANES analysis of oxides at the nanoscale. IUCrJ **1**, 571–589 (2014). https://doi.org/10.1107/S2052252514021101
40. P. Strunz, D. Mukherji, G. Pigozzi, et al., Characterization of core-shell nanoparticles by small angle neutron scattering. Appl. Phys. A Mater. Sci. Process. **88**, 277–284 (2007). https://doi.org/10.1007/s00339-007-4008-7
41. S. Mühlbauer, D. Honecker, É.A. Périgo, et al., Magnetic small-angle neutron scattering. Rev. Mod. Phys. **91**, 1–75 (2019). https://doi.org/10.1103/revmodphys.91.015004
42. M. Bersweiler, P. Bender, L.G. Vivas, et al., Size-dependent spatial magnetization profile of manganese-zinc ferrite M n0.2 Z n0.2 F e2.6 O4 nanoparticles. Phys. Rev. B **100**, 1–10 (2019). https://doi.org/10.1103/PhysRevB.100.144434
43. M. Bonini, A. Wiedenmann, P. Baglioni, Small angle polarized neutrons (SANSPOL) investigation of surfactant free magnetic fluid of uncoated and silica-coated cobalt-ferrite nanoparticles. J. Phys. Chem. B **108**, 14901–14906 (2004). https://doi.org/10.1021/jp049286a
44. S. Brice-Profeta, M.-A. Arrio, E. Tronc, et al., Magnetic order in γ-Fe2O3 nanoparticles: a XMCD study. J. Magn. Magn. Mater. **288**, 354–365 (2005). https://doi.org/10.1016/j.jmmm.2004.09.120
45. R. Russo, E. Esposito, C. Granata, et al., Magnetic nanoparticle characterization using nano-SQUID based on niobium Dayem bridges. Phys. Procedia **36**, 293–299 (2012). https://doi.org/10.1016/j.phpro.2012.06.162

46. L. Angeloni, D. Passeri, S. Corsetti, et al., Single nanoparticles magnetization curves by controlled tip magnetization magnetic force microscopy. Nanoscale **9**, 18000–18011 (2017). https://doi.org/10.1039/C7NR05742C
47. M. Kim, C.S. Kim, H.J. Kim, et al., Effect hyperthermia in CoFe2O4@MnFe2O4 nanoparticles studied by using field-induced Mossbauer spectroscopy. J. Korean Phys. Soc. **63**, 2175–2178 (2013). https://doi.org/10.3938/jkps.63.2175
48. S. Mørup, Mössbauer effect in small particles. Hyperfine Interact. **60**, 959–973 (1990). https://doi.org/10.1007/BF02399910
49. S. Mørup, H. Topsøe, B.S. Clausen, Magnetic properties of microcrystals studied by mössbauer spectroscopy. Phys. Scr. **25**, 713–719 (1982). https://doi.org/10.1088/0031-8949/25/6A/015
50. J. Fock, M.F. Hansen, C. Frandsen, S. Mørup, On the interpretation of Mössbauer spectra of magnetic nanoparticles. J. Magn. Magn. Mater. **445**, 11–21 (2018). https://doi.org/10.1016/j.jmmm.2017.08.070
51. I.P. Suzdalev, Magnetic phase transitions in nanoclusters and nanostructures. Russ. J. Inorg. Chem. **54**, 2068 (2009). https://doi.org/10.1134/S0036023609130038
52. D.H. Jones, K.K.P. Srivastava, Many-state relaxation model for the Mössbauer spectra of superparamagnets. Phys. Rev. B **34**, 7542–7548 (1986). https://doi.org/10.1103/PhysRevB.34.7542
53. M. Blume, J.A. Tjon, Mössbauer spectra in a fluctuating environment. Phys. Rev. **165**, 446–456 (1968). https://doi.org/10.1103/PhysRev.165.446
54. U. Gonser, F. Aubertin, S. Stenger, et al., Polarization and thickness effects in Mössbauer spectroscopy. Hyperfine Interact. **67**, 701–709 (1991). https://doi.org/10.1007/BF02398222
55. B. Kalska-Szostko, M. Cydzik, D. Satula, M. Giersig, Mossbauer studies of core-shell nanoparticles. Acta Phys. Pol. A **119**, 15–17 (2011). https://doi.org/10.12693/APhysPolA.119.15
56. A. Chuev, Mössbauer spectra and magnetization curves of nanoparticles in a weak magnetic field. J. Phys. Conf. Ser. **217**, 8–12 (2010). https://doi.org/10.1088/1742-6596/217/1/012011
57. S.D. Oberdick, A. Abdelgawad, C. Moya, et al., Spin canting across core/shell Fe3O4/MnxFe3−xO4 nanoparticles. Sci. Rep. **8**, 3425 (2018). https://doi.org/10.1038/s41598-018-21626-0
58. B. Pacakova, S. Kubickova, A. Mantlikova, et al., Spinel ferrite nanoparticles: Correlation of structure and magnetism, in *Magnetic Spinels- Synthesis, Properties and Applications*, (InTech, London, 2017)
59. S.J. Iyengar, M. Joy, C.K. Ghosh, et al., Magnetic, X-ray and Mossbauer studies on magnetite/maghemite core-shell nanostructures fabricated through an aqueous route. RSC Adv. **4**, 64919–64929 (2014). https://doi.org/10.1039/c4ra11283k
60. A.S. Kamzin, I.M. Obaidat, A.A. Valliulin, et al., Mossbauer studies of the structure of core/shell Fe3O4/-Fe2O3 nanoparticles. Tech. Phys. Lett. **45**, 426–429 (2019). https://doi.org/10.1134/S1063785019050079
61. A.S. Kamzin, A.A. Valiullin, H. Khurshid, et al., Mossbauer studies of core-shell FeO/Fe3O4 nanoparticles. Phys. Solid State **60**, 382–389 (2018). https://doi.org/10.1134/S1063783418020129
62. A. Lak, M. Kraken, F. Ludwig, et al., Size dependent structural and magnetic properties of FeO-Fe 3O4 nanoparticles. Nanoscale **5**, 12286–12295 (2013). https://doi.org/10.1039/c3nr04562e
63. E.C. Sousa, H.R. Rechenberg, J. Depeyrot, et al., In-field Mossbauer study of disordered surface spins in core/shell ferrite nanoparticles. J. Appl. Phys. **106**, 93901 (2009). https://doi.org/10.1063/1.3245326
64. S. Kubickova, J. Vejpravova, P. Holec, D. Niznansky, Correlation of crystal structure and magnetic properties of $Co_{(1-x)}Ni_xFe_2O_4/SiO_2$ nanocomposites. J. Magn. Magn. Mater. **334**, 102 (2013). https://doi.org/10.1016/j.jmmm.2013.01.005
65. A. Repko, D. Nižňanský, J. Poltierová-Vejpravová, A study of oleic acid-based hydrothermal preparation of CoFe2O4nanoparticles. J. Nanopart. Res. **13**, 5021–5031 (2011). https://doi.org/10.1007/s11051-011-0483-z
66. J. Vejpravová, V. Sechovsky, J. Plocek, et al., Magnetism of sol-gel fabricated Co Fe_2O_4Si O_2 nanocomposites. J. Appl. Phys. **97**, 124304 (2005). https://doi.org/10.1063/1.1929849

67. G. Concas, G. Spano, C. Cannas, et al., Inversion degree and saturation magnetization of different nanocrystalline cobalt ferrites. J. Magn. Magn. Mater. **321**, 1893–1897 (2009). https://doi.org/10.1016/j.jmmm.2008.12.001
68. M. Siddique, N.M. Butt, Effect of particle size on degree of inversion in ferrites investigated by Mössbauer spectroscopy. Phys. B Condens. Matter **405**, 4211–4215 (2010). https://doi.org/10.1016/j.physb.2010.07.012
69. J. Kurian, S.P. John, M.M. Jacob, et al., Mössbauer studies of nanocrystalline ZnFe2O4 particles prepared by spray pyrolysis method. IOP Conf. Ser. Mater. Sci. Eng. **73**, 012032 (2015). https://doi.org/10.1088/1757-899X/73/1/012032
70. N. Moumen, P. Bonville, M.P. Pileni, Control of the size of cobalt ferrite magnetic fluids: Mössbauer spectroscopy. J. Phys. Chem. **100**, 14410–14416 (1996). https://doi.org/10.1021/jp953324w
71. K.M. Batoo, D. Salah, G. Kumar, et al., Hyperfine interaction and tuning of magnetic anisotropy of Cu doped CoFe2O4 ferrite nanoparticles. J. Magn. Magn. Mater. **411**, 91–97 (2016). https://doi.org/10.1016/j.jmmm.2016.03.058
72. N. Lakshmi, H. Bhargava, O.P. Suwalka, et al., Magnetic properties resulting from core-shell interactions in nanosized Ni0.25 Co0.25 Zn0.5 Fe2 O4. Phys. Rev. B Condens. Matter Mater. Phys. **80**, 1–6 (2009). https://doi.org/10.1103/PhysRevB.80.174425
73. S. Burianova, J. Poltierova Vejpravova, P. Holec, et al., Surface spin effects in La-doped $CoFe_2O_4$ nanoparticles prepared by microemulsion route. J. Appl. Phys. **110**, 073902 (2011). https://doi.org/10.1063/1.3642992
74. S. Burianova, J.P. Vejpravova, P. Holec, et al., Observation of surface effects in La-doped CoFe2O 4/SiO2 nanocomposites. IOP Conf. Ser. Mater. Sci. Eng. **18**, 022015 (2011)
75. M.S. Angotzi, A. Musinu, V. Mameli, et al., Spinel ferrite core-shell nanostructures by a versatile solvothermal seed-mediated growth approach and study of their nanointerfaces. ACS Nano **11**, 7889–7900 (2017). https://doi.org/10.1021/acsnano.7b02349
76. Z. Zhao, H. Cui, W. Song, et al., A simple magnetic nanoparticles-based viral RNA extraction method for efficient detection of SARS-CoV-2. *bioRxiv*, 518055:2020.02.22.961268 (2020). https://doi.org/10.1101/2020.02.22.961268